A. REMARKS

Claims 1-4, 6-9, 20-23 remain pending. Claims 24-26 are added by this response. No new matter is added by the newly presented claims.

B. Rejections under 35 U.S.C. 112

Claims 1-4, 6-9 and 20-23 were rejected under 35 U.S.C. 112, second paragraph, as being indefinite because the specification does not explain how the axial dispersion coefficient would be determined in a given system.

The Applicants respectfully submit that by the term "axial dispersion coefficient," they do not seek any special or broader definition than that accorded to the term by one of skill in the art and that this is a term of art that is well substantiated as explained below. Use of this term in the Applicants' specification and claims is consistent with the ordinary and accepted meaning of this term.

In order to determine whether or not a given process falls within the metes and bounds of the claims (specifically, whether a given process is conducted in a manner that yields a plug flow index of more than 50), one would only need to measure or model the axial dispersion coefficient for a particular implementation. A variety of techniques are known for measuring and modeling axial dispersion coefficient. As a illustration of the methods known in the art for determining axial dispersion coefficient applicable to the application, please see the following references and references cited therein (i) pages 529-531 and 532-551, Chemical Reactor Analysis and Design, 2nd Edition, Gilbert Froment and Kenneth Bischoff, John Wiley & Sons, NY; ISBN 0-471-51044-0; (publication year: 1990); (ii) pages 2248-2250, Axial Dispersion in a Kureha Crystal Purifier, K Otawara and T Matsuoka, Journal of Crystal Growth, Volume 237-239 (publication year: 2002); (iii) pages 41-51, Reactor Models, S Dutta and R Gualy, Chemical Engineering Progress, (publication year: October 2000). While these references teach specific techniques, any method now known or later discovered may be used to quantify the axial dispersion coefficient which, in turn, can be used to determine whether a particular process is falls within the scope of the instant claims.
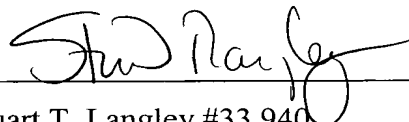
C. Conclusion

In view of all of the above, claims 1-4, 6-9 and 20-26 are believed to be allowable and the case in condition for allowance which action is respectfully requested. The references that were cited and not relied upon are believed to be no more pertinent that those references that were relied upon.

No fee is believed to be required by this response as determined on the accompanying transmittal letter. Should any other fee be required, please charge Deposit 50-1123. Should any extension of time be required please consider this a petition therefore and charge the required fee to Deposit Account 50-1123.

Respectfully submitted,

Date: <u>November 3, 2003</u>   BY:_____

Stuart T. Langley #33,940
HOGAN & HARTSON LLP
One Tabor Center
1200 17th Street, Suite 1500
Denver, Colorado 80202
Phone: (720) 406-5335
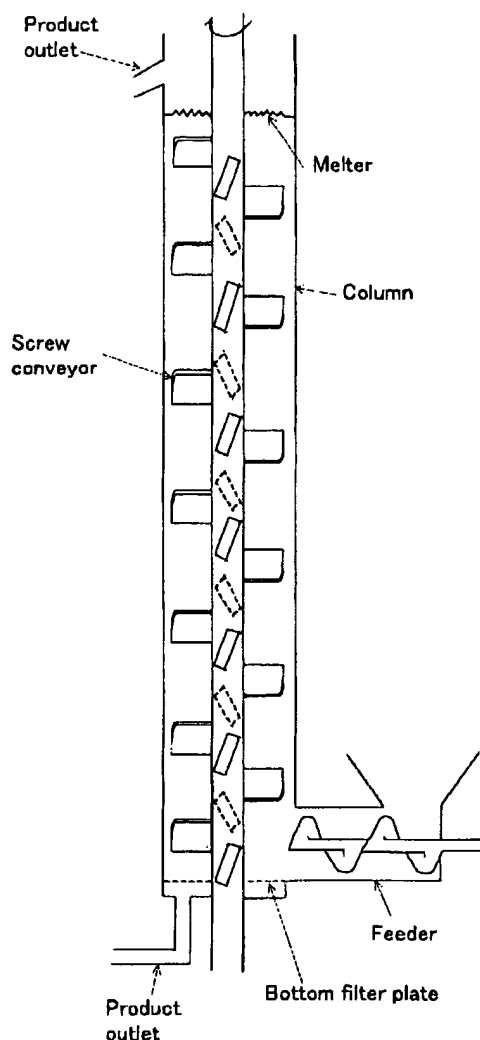Fax: (720) 406-5301

References attached (9 pages)

Fig. 2. Structure of a KCP.

product exits as crystal from the top of the column. Typical usage of a KCP is depicted in Fig. 3.

3. Theoretical

For scaling up the KCP, the following two phase counter current dispersion model [5] has been adopted as the steady state model.

$$E_x \frac{d^2 C_x}{dz^2} + V_x \frac{dC_x}{dz} + k_a C_y = 0, \tag{1}$$

$$E_y \frac{d^2 C_y}{dz^2} - V_y \frac{dC_y}{dz} - k_a C_y = 0. \tag{2}$$

The boundary condition is expressed as

$$-E_x \left(\frac{dC_x}{dz}\right)_{z=L} = V_x(C_{xz \to L} - C_{xT}) \text{ at } z = L, \tag{3}$$

$$\frac{dC_x}{dz} = 0 \quad \text{at } z = 0, \tag{4}$$

$$-E_y \left(\frac{dC_y}{dz}\right)_{z \to 0} = V_y(C_{yB} - C_{yz \to 0}) \text{ at } z = 0, \tag{5}$$

$$\frac{dC_y}{dz} = 0 \quad \text{at } z = L, \tag{6}$$

where C, V, E, k_a, x, and y are concentration of impurities, velocity, axial dispersion coefficient, sweating rate constant, liquid, and solid, respectively. The model simplified various aspects of phenomena in the KCP: For example, temperature profile along the axis, recrystallization, size distribution of crystals or washing effect is not taken into account. Currently, we are trying to develop models which incorporate more details of such phenomena than the present model. This will be reported in the future.

The model has three parameters, i.e., sweating rate constant and axial dispersion coefficients for liquid and solid. Among these, axial dispersion coefficients can be estimated by well-known tracer technique as discussed in the succeeding section. The sweating rate constant has been estimated by analyzing impurity concentration profile along the axis. This will be published elsewhere.

4. Experimental procedure

To estimate axial dispersion coefficients and mean velocities of liquid, tracer technique experiments have been carried out for obtaining residence time distributions of liquid with the variations of the size of the KCP.

When an idealized tracer pulse is introduced into a vessel with the boundary condition of the closed system, an axial dispersion coefficient can
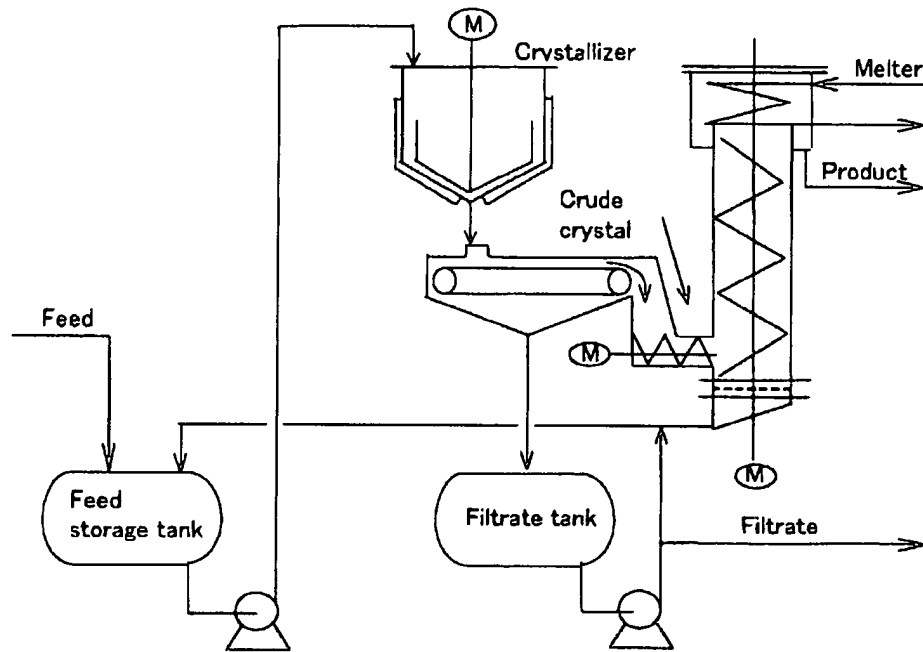
Fig. 3. Representative flow diagram of a KCP system.

be calculated by (see, e.g., [6])

$$\sigma_0^2 = 2\frac{E}{uL} - 2\left(\frac{E}{uL}\right)^2 (1 - e^{-uL/E}), \tag{7}$$

where σ_0 is the normalized standard deviation for the tracer response at the exit of the vessel.

Monochlorobenzene has been chosen as a tracer. Its temperature has been kept around the melting point of para-dichlorobenzene (p-DCB) to minimize the disturbance to the operation of the KCP. A certain amount of the tracer, e.g., 1 kg for the KCP of 0.51 m in diameter, has been fed as a pulse input from the top of the column after the KCP was stabilized to produce pure p-DCB. Then, the bottom product has been sampled every 3 min and its composition has been analyzed by a gas chromatography. To estimate the effect of the column diameter on the axial dispersion coefficient, the similar experiments have been carried out for KCPs of 0.08 and 0.15 m in diameter as well with less amount of the tracer.
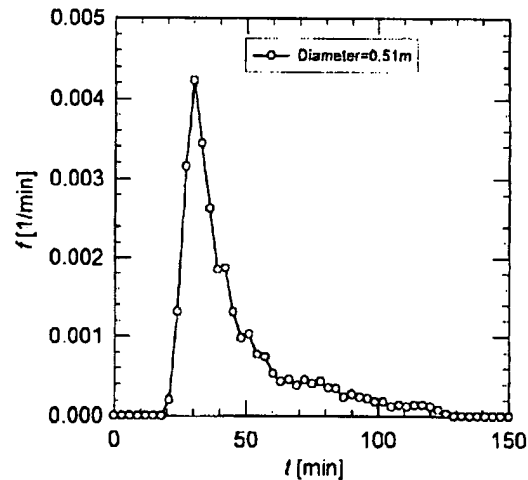

Fig. 4. Residence time distribution of tracer as the liquid phase in the KCP.

5. Results and discussion

Fig. 4 illustrates the composition profile of the tracer of the sample taken from the bottom of a KCP whose diameter is 0.51 m. It appears that the flow of liquid phase in the KCP is not totally plug
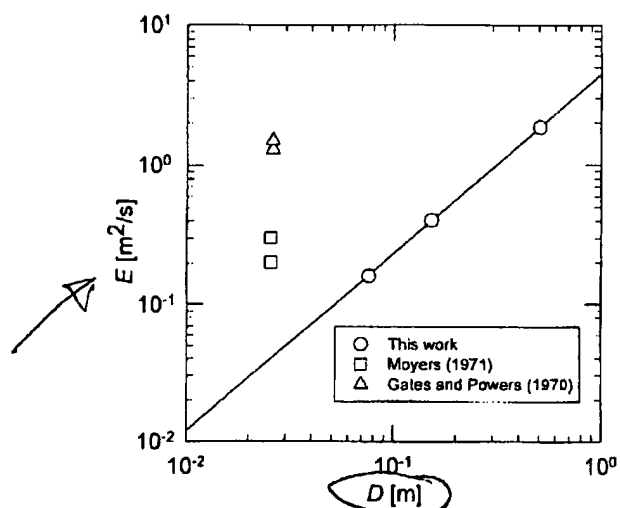
Fig. 5. Comparison of axial dispersion coefficients of liquid with a variation of inner diameter of crystallization columns.

flow, but has a small degree of the back-mixing. The axial dispersion coefficient, i.e., E, of KCP with the variation of the column diameter, i.e., D, of the KCP is shown in Fig. 5. From this, the following relation between the size of the diameter of the KCP and the axial dispersion of the liquid phase in the KCP has been derived.

$$E = k_E D^{1.29}. \qquad (8)$$

In this expression, k_E is a proportional constant. This indicates that the larger the KCP is, the more significant the axial dispersion is. Fig. 5 also shows that the axial dispersion in the KCP can be substantially smaller than those reported for other types of column crystallizer for a given column diameter [7–8]. Thus, KCP might possibly outperform them especially when their diameters are large.

Experiments to investigate the axial dispersion coefficients of the solid phase have been executed for KCPs with the column diameter of 0.08 and 0.15 m. Nevertheless, so far there has been no opportunity for such experiments using KCPs of industrial sizes, since solid tracer, which are proved to be not harmful to p-DCB and KCP processes, have not been found at this moment. The axial dispersion coefficients of the solid phase will be explored and reported in the future. Nevertheless, we have carried out experiments

with KCPs of 0.08 and 0.15 m in diameter and have obtained rough effect of the column diameter on the axial dispersion coefficients in the solid phase.

In designing the KCPs, it is most important to determine their column heights. With the model discussed in the theoretical session, if we estimate parameters included in the model by the experimental correlation equation obtained in Fig. 5 and the allowable concentration of impurities of the product is specified, the required heights can be calculated. The largest KCPs, specifically, 0.76 m in column diameter, were constructed in 1998 in this manner. These KCPs have been successfully operated and their capacities for purifying p-DCB have been proved to be 13,000 T/y. Small axial dispersion coefficients have rendered possible to develop such KCPs.

6. Concluding remarks

The axial back-mixing in the equipment affects the performance of a column crystallizer. In this paper, the axial dispersion of the liquid phase in the KCP has been investigated and it is found how the diameter of the KCP affects the axial dispersion coefficient of the KCP. These coefficients have been compared to those obtained for other types of column crystallizers and it has been found that the former is substantially smaller than the latter.

References

[1] D.L. McKay, H.W. Goard, Chem. Eng. Progress 61 (1965) 99.

[2] J.A. Brodie, Mech. Chem. Eng. Trans., Inst. Eng. Aust. (1971) 37.

[3] D.H. Joseph Jr., et al., in: R.H. Perry, D. Green (Eds.), Perry's Chemical Handbook Vol. 7, McGraw-Hill, New York, 1984, pp. 7–10.

[4] K. Sakuma, Aromatikusu 37 (1985) 109 (in Japanese).

[5] T. Miyauchi, T. Vermeulen, Ind. Eng. Chem. Fundam. 2 (1963) 113.

[6] O. in: Levenspiel (Ed.), Chemical Reaction Engineering, 2nd Edition, Wiley, New York, 1962, p. 276.

[7] W.C. Gates Jr., J.E. Powers, AIChE J. 16 (1970) 648.

[8] C.G. Moyers Jr., Ph.D. Thesis, University of Delaware, Newark, 1971.

grams usually cover deflagration, which is caused by sudden gas expansion by an accelerated reaction. The maximum pressure buildup due to such an explosion can be estimated from the pressure/volume relationship of the complete reaction/combustion process. The detonation process, on the other hand, is more violent, generating shock waves that travel at a speed several orders of magnitude higher than the pressure wave caused by deflagration. The local pressure buildup from this phenomenon, thus, is substantially higher — for most hydrocarbon/air mixtures, about 15–20 times the initial pressure, compared to a maximum of two times in case of deflagration. See, for example, Ref. 6 for details on these explosion phenomena.

Therefore, the detonation characteristics of the reaction mixture should be studied, along with deflagration, to address reactor safety more thoroughly.

STEP 6 — DEFINE REACTOR TYPE AND ITS HYDRODYNAMICS.
The reactor type is defined by: (a) the physical configuration of the volume occupied by the reaction system; (b) the flow mode of various streams in and out of the reactor; and (c) the hydrodynamic representation of the flows within the reactor volume. Thus, for example, a CSTR usually represents a stirred vessel with continuous flow of a homogeneous fluid stream or continuous phase in and out of the vessel. The hydrodynamic representation of a CSTR assumes the fluid stream is completely mixed as soon as it enters the vessel and attains the outlet composition instantaneously. A PFR embodies the other extreme. It usually is tubular (with a high ratio of length, L, to diameter, D) in configuration. The flow in and out this reactor type is the same as that in the CSTR. The representation of the PFR hydrodynamics, however, assumes a total absence of axial mixing of the flowing streams within the reactor.

A homogeneous reactor usually is

designed using the performance equations of either the CSTR or PFR. This allows easier analysis, design, and scale-up of such reactors. But, these idealized reactors do not closely enough mirror the behavior of a real reactor. Such a reactor is better represented by a system with axial dispersion or by an axially dispersed reactor (ADR), the performance of which falls between that of a CSTR and a PFR. For a simple first-order reaction, A → B, the steady-state mass-balance equation of an ADR can be described as:

$$D_a \frac{d^2 c_A}{dz^2} - u \frac{dc_A}{dz} - kc_A = 0 \qquad (1)$$

where D_a is the axial dispersion coefficient.

The predicted behavior of the ADR approaches that of a PFR for no axial dispersion, i.e., $D_a = 0$, and that of a CSTR for infinite dispersion (complete mixing), i.e., $D_a = \infty$. For a real reactor, D_a is a finite number greater than zero.

In developing a robust model, it may be advisable to start with an ADR equation, rather than a CSTR or PFR one. For initial model development, the ADR equation can be turned into simple CSTR or PFR ones by substituting the two limiting values of D_a. But, including the D_a term allows you to fine-tune the model at a later stage to predict the reactor performance more precisely. To use this approach, however, the value of D_a needs to be determined by experiment or from one of the many correlations available in literature, for example, in Refs. 1–4 and 7–10. These correlations usually are available in the form of the dimensionless Peclet number, N_{Pe} (= Lu/D_a, where L and u represent tube length and fluid velocity, respectively). The Peclet number typically is expressed as a function of Reynolds number, N_{Re}, which represents the flow behavior within the reactor. $N_{Pe} > 100$ normally indicates an approach to the behavior of a PFR, while $N_{Pe} < 1$ to that of a CSTR. Qualitatively, a longer tube length or

higher fluid velocity means more PFR-like performance, and the reverse more CSTR-like.

The above discussions are for continuous flow reactors. For both homogeneous and heterogeneous reactors, however, part of the reaction mixture or one or more of the phases can be captive or in nonflow condition, while the rest can be in continuous or intermittent flow mode. Reactants can be injected along the reactor length or reactor path in the case of multiple-reactor systems. The reactor product can be recycled with the reactor feed before or after separation stages. These represent batch, semi-batch, multi-injection, and recycle reactor types. For heterogeneous reactors, the flow of the phases can be co- or counter-current.

For gas/solid reactors, the gas usually is in a continuous flow mode. The solid, however, can remain fixed in position within the reactor through which the gas percolates. Or, both solid and gas can flow continuously in co- or counter-current mode through the reactor. With the solid remaining fixed within the reactor, there are again various reactor types — for example, the nonadiabatic packed-bed tubular reactor (NAPB-TR), adiabatic packed-bed multistage reactor (APBMSR), monolithic reactor, and radial flow reactor. An APBMSR can be operated with direct quench (interstage cooling or heating) by feed or recycle-gas injection or indirect quench by a heat exchanger. For continuous flow of both gas and solid, the possible reactor types include moving bed (co- and counter-current), bubbling and turbulent fluidized beds, circulating and fast fluidized beds, and entrained beds.

For gas/liquid systems, the reactor generally used is either a stirred tank or a bubble column. The bubble column can be vertically or horizontally sparged, vertical or horizontal flow, gas-lifted (internally or externally), and with or without a forced liquid-circulation loop. The bubble columns also can be categorized according to

Chemical Reactor Analysis and Design

Second Edition

Gilbert F. Froment

Rijksuniversiteit Gent, Belgium

Kenneth B. Bischoff

University of Delaware

WILEY

John Wiley & Sons

New York · Chichester · Brisbane · Toronto · Singapore

is a function
ey observed
ied between
o 3600 rpm.
and was 1.9

even more
n (especially
be quite im-
is where the
nditions are

confirmed:
n, and con-
l, and Adler

:inciple, but
lesser order
o-use segre-
l to predict
mixing. For
some of the
eral method

te levels of
ders the re-
ate and one
ermaux and
reactor data
es between
elements as
i the popu-
in that only
give similar
at of Viller-
"interaction
xperimental
t-no general

oases of the
nents [Beck
that the ul-
i molecular
mixing and/
n time, and
to the ma-
macrotime,
t-order rate
ic diffusion
ctor, allow-
d in a fluid

Similar approaches have been taken by Truong and Methot (1976). Also, Danckwerts (1958) defined an index of segregation based on the variances of the ages in the fluid elements and the vessel as a whole; however, there is no direct relation with reactor performance.

Again, no general correlations of these parameters are available. Surveys of various aspects of relating turbulent mixing concepts to micromixing in reactors appear in Brodkey (1975). Surveys of the topic of mixing and chemical reactions are given by Olson and Stout (1966) and by Villermaux (1976a, 1986b).

A final important point is that all of the above is valid only for isothermal conditions in single-phase systems. Extension to other cases requires the introduction of interactions with the second phase and/or heat exchange walls, for example, and the age distribution and micromixing functions depend much more on the details of the system. A formal treatment would use joint probability distribution functions, but this rapidly gets extremely complex. The population balance models can give some insight into the two-phase situation. They are discussed below.

12.6
MODELS ACCOUNTING
FOR FLOW PATTERNS

12.6.1 Axial Dispersion Model
and Tanks-in-Series Model

The above methods are quite general in that they are not based on any specific physical model. On the other hand, they are limited in presuming that the RTD is available and also by restriction to homogeneous phases. Thus, other techniques are required for predictive purposes and design where the actual reactor is obviously not available for a tracer test. To develop general correlations of behavior, the usual engineering tactics of utilizing mathematical models with parameters to be determined from the experimental data are useful. These parameters are then correlated as functions of fluid and flow properties, reactor configurations, along with other important features, and can be used in design calculations. The flow models are semiempirical in nature, but hopefully will bear some relation to the actual flow patterns in the vessel.

There are several types of models that have found useful applications, but two are most common—at least when found to be adequate to represent the physical situation. The first is usually termed the "axial dispersion" or "axial dispersed plug flow" model [Levenspiel and Bischoff (1963)] and takes the form of the one-dimensional diffusion equation with a convective term. The second is a series of perfectly mixed vessels, some features of which have been discussed in Sec. 12.3.

The mass balance for the axial dispersion model is, from Chapter 7,

$$\frac{\partial c}{\partial t} + u\frac{\partial c}{\partial z} = \frac{\partial}{\partial z} D_a \frac{\partial c}{\partial z} + r(c) \tag{12.6.1-1}$$

In Eq. 12.6.1-1, u is taken to be the mean (plug flow) velocity through the vessel, and D_a is a mixing-dispersion coefficient to be found from experiments with the system of interest. One important application is to fixed beds, as discussed in detail in Chapter 11, and then it is usually termed an "effective" transport model, with $D_a = D_{ea}$. However, the axial dispersion model can also be used to approximately describe a variety of other reactors.

One of the main benefits of this model is its analogy to the diffusion equation, and the possibility of utilizing all of the classical mathematical solutions that are available [e.g., Carslaw and Jaeger (1959) and Crank (1956)].

One common approach to determining the model parameter D_a is to perform a residence time distribution test on the reactor and to choose the value of D_a so that the model solution and experimental output curve agree [e.g., by least squares techniques (see Sec. 12.6.3)]. Figure 12.6.1-1 shows the $E(\theta')$–θ' curves of the model for an impulse input with "closed" boundaries (here, $\theta' = \theta F'/V = \theta u/L$, with L = length of the reactor):

$$\frac{C}{M/V} = E(\theta') = e^{Pe_a/2} \sum_{i=1}^{\infty} \frac{(-1)^{i+1} 8\alpha_i^2}{4\alpha_i^2 + 4Pe_a + Pe_a^2} \times \exp\left[\frac{-\theta'(Pe_a^2 + 4\alpha_i^2)}{4Pe_a}\right] \quad (12.6.1\text{-}2)$$

with α_i positive roots of

$$\tan \alpha_i = \frac{4Pe_a\alpha_i}{4\alpha_i - Pe_a^2}$$

or

$$\left(\frac{\alpha_i}{2}\right) \tan\left(\frac{\alpha_i}{2}\right) = \frac{Pe_a}{4} \qquad \left(\frac{\alpha_i}{2}\right) \cot\left(\frac{\alpha_i}{2}\right) = -\frac{Pe_a}{4}$$
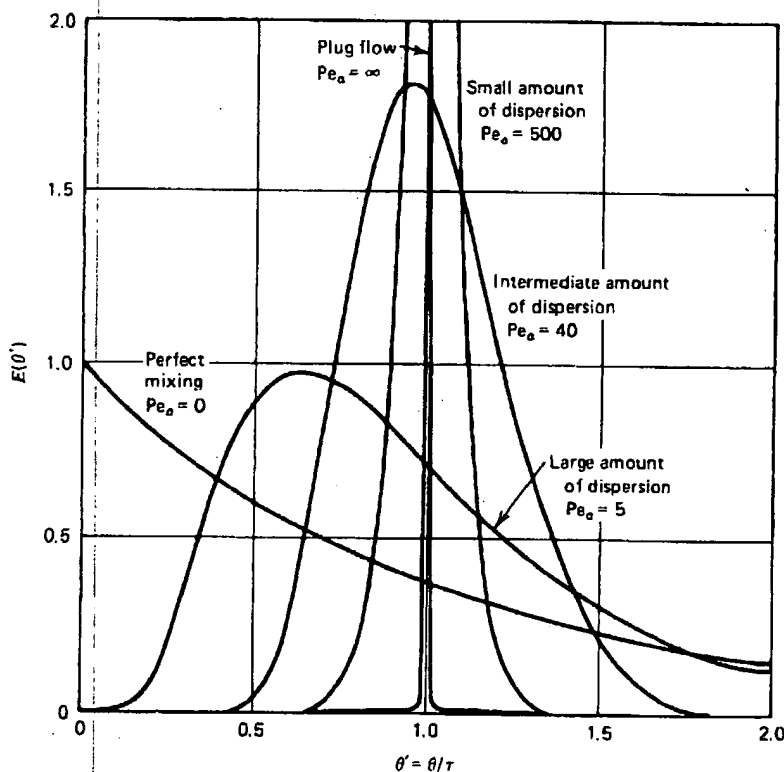
where

$$Pe_a = uL/D_a.$$

Figure 12.6.1-1
E curves in closed vessels for various extents of dispersion: $Pe_a = uL/D_a$. After Levenspiel (1972).

he diffusion
cal solutions
)].
ter D_a is to
choose the
curve agree
5.1-1 shows
boundaries

$$\Bigg] \qquad (12.6.1\text{-}2)$$

[See Carslaw and Jaeger (1956).] A thorough evaluation was given by Brenner (1962). It is seen that the axial dispersion model can represent mixing behavior ranging from perfect mixing ($D_a \to \infty$) to plug flow ($D_a \to 0$).

Other types of boundary conditions can also be used when solving Eq. 12.6.1-1 (some details are given below when discussing chemical reactor applications); for example, in an "infinite" pipe, the dispersion characteristics upstream from the tracer injection would be identical to those within the system, and a different mathematical solution results:

$$\frac{C}{M/V} = E(\theta') = \frac{1}{2}\left(\frac{Pe_a}{\pi\theta'}\right)^{1/2} \exp\left[-\frac{Pe_a(1 - \theta')^2}{4\theta'}\right] \qquad (12.6.1\text{-}3)$$

The E curves from Eq. 12.6.1-3 are similar to those from Eq. 12.6.1-2 for reasonably large values of Pe_a.

Many of the available solutions are given in Levenspiel and Bischoff (1963), Himmelblau and Bischoff (1968), and Wen and Fan (1975). As a practical matter, these mathematical complexities should probably not be taken too literally because the precise conditions at the boundaries of real equipment cannot usually be exactly defined, in any event. That is, if the boundary condition details give significantly different results, be cautious about the axial dispersion model as being a faithful representation of the flow patterns in the vessel. These differences are only seen for large values of D_a (actually, small Pe_a), but the physical basis is a diffusionlike situation, which would not be valid for extremely large levels of mixing.

EXAMPLE 12.6.1.1
AXIAL DISPERSION MODEL FOR LAMINAR FLOW IN ROUND TUBES

This is one situation where the exact convective diffusion equation can be solved and compared with the one-dimensional dispersion equation. The complete equation is

$$\frac{\partial C}{\partial t} + 2u\left(\frac{R^2 - r^2}{R^2}\right)\frac{\partial C}{\partial z} = \mathscr{D}\left(\frac{1}{r}\frac{\partial}{\partial r}r\frac{\partial C}{\partial r} - \frac{\partial^2 C}{\partial z^2}\right) \qquad (a)$$

where u is the mean velocity.

Taylor (1953) has discussed this in detail, and a summary of the results is given here. Taylor and Aris (1956) showed that the main variable of interest, the mean concentration, is

$$\langle C \rangle = \frac{2}{R^2}\int_0^R rC\,dr$$

could be found by averaging Eq. (a) (for impermeable walls):

$$\frac{\partial \langle C \rangle}{\partial t} + u\frac{\partial \langle C \rangle}{\partial z} = \mathscr{D}\frac{\partial^2 \langle C \rangle}{\partial z^2} - \frac{4u}{R^4}\frac{\partial}{\partial z}\int_0^R [C(r) - \langle C \rangle]r^3\,dr \qquad (b)$$

$$\sim D_a\frac{\partial^2 \langle C \rangle}{\partial z^2} \qquad (c)$$

with

$$D_a = \mathscr{D} + \frac{1}{48}\frac{u^2 R^2}{\mathscr{D}} \qquad (d)$$

See Hunt (1977) for a more recent exposition. The step from Eq. (b) to Eq. (c) is only possible under conditions that the radial concentration profile has a